Add to Section 1.3.1, p 11, as last paragraph.

A detailed model of muscular contraction appears in Smith et al., (2008). This model integrates the biochemical and biomechanical aspects of actinomyosin contraction. Such details are beyond the scope of this text.

ref:

Smith, D. A., M. A. Greeves, J. Sleep, and S. M. Mijailovich, 2008, Towards a Unified Theory of Muscle Contraction. I: Foundations, *Ann. Biomed. Engr*. 36(10): 1624-1640.

Add to Section 2.2.3, before paragraph beginning "Not only do the joints. . . ,p. 70.

Bone mineral density has a large impact on bone strength, and bone mineral density decreases with age. Women, in particular, are in danger of critical bone strength reduction due to osteoporosis. Fracture load averages about 6000 N for the L3* vertebra up until age 40, but decreases linearly thereafter at about 500 N/decade of life (Nelson et al., 2009).

Astronauts, too, are at risk for bone fracture because bone density decreases about 17% per month in space (Nelson, et al., 2009). Nelson et al., (2009) developed a probabalistic model of bone fracture risk for space travelers to the moon and Mars. Their model predicted low fracture risks for short moon missions, but much higher risks for a longer Mars mission. Wrist fracture was the most likely type of fracture, followed by spinal and hip fracture.

Reference:

Nelson, E. E., B. Lewandowski, A. Licata, and J. G. Myers, 2009, Development and Validation of A Predictive Bone Fracture Risk Model for Astronauts, *Ann. Biomed. Engr*. 37:2337-2359.

*The spinal column is classified into five vertebral regions: cervical, dorsal, lumbar, sacral, and coccygeal. The lumbar portion is located in the lower back. The L3 vertebra refers to the third of five lumbar vertebra.

add to index

Osteoporosis

Astronaut bone strength

Bone Fracture

Add to Section 3.2.1, as second to last paragraph:

The normal percentage hematocrit in men is in the mid 40s. Trained endurance athletes can increase their sustained natural percentage hematocrit to the high 40s or low 50s. Injecting the hormone erythropoietin can result in hematocrit percentages in the high 50s or low 60s. Such an increase in the number of red blood cells in the body can vastly increase oxygen-carrying capacity and increase physical performance by 5-10%. However, blood with a hematocrit of 60 percent or higher becomes thick and easily clotted (Shermer, 2008).

Ref:

Shermer, M., 2008, The Doping Dilemma, *Sci. Amer.* 298(4): 82-89 (Apr).

Add to Section 3.2.1, as next to last paragraph beginning "Exercising individuals exhibit. . . ″, p. 128.

Red blood cells normally form reversible aggregates when flow rate is slow, but are torn apart and return to individual cells when flow rate increases (Fenech et al., 2009). Erythrocyte aggregation is almost totally responsible for non-Newtonian flow behavior of blood.

Reference:

Fenech, M., D. Garcia, H. J. Meiselman, and G. Cloutier, 2009, A Particle Dynamic Model of Red Blood Cell Aggregation Kinetics, *Ann. Biomed. Engr*. 37: 2299-2309

add to index:

Blood cell aggregates

non-Newtonian flow

Add to Section 3.31, after the sentence ending with" . . maintaining homeostasis of the brain.", p. 164.

A model of this brain blood autoregulation can be found in Payne et al., (2009).

Reference:

Payne, S. J., J. Selb, and D. A. Boas, 2009, Effects of Autoregulation and CO_2 Reactivity on Cerebral Oxygen Transport, *Ann. Biomed. Engr.* 37:2288-2298,

add to index:

Blood flow, brain

Brain blood flow

autoregulation, blood flow

Add to Section 3.3.2, as last paragraph:

Nitric oxide circulating in the blood is a significant factor in keeping small blood vessels open, and allowing them to provide oxygen-rich blood to working muscle. Without this nitric oxide, tissues can be starved for oxygen and the risk of heart attacks can increase by 15% or more. This sometimes happens with transfused blood (Mossman, 2007; Park, 2007).

Ref:

Mossman, K., 2007, Crucial Factor Declines in Banked Blood. *Proc.Nat.Acad.Sci.* 104(43): 16721-16722.

Park, A., 2007, The Problem with Transfusions, *Time* 170(17):56 (22 Oct).

3.4.6 Vascular Flow Model

Computational simulations of vascular blood flow can be used when experimental data is limited or unavailable. They are used for the design and evaluation of vascular medical devices, planning of vascular surgeries, and predictions of outcomes.

Kim et al. (2009) have formulated a model of the aorta in which they coupled upstream left ventricular lumped-parameter characteristics and downstream lumped-parameter Windkessel vessel characteristics to the three dimensional finite element description of the aorta (Figure 3.4.15). The lumped-parameter heart model consists of an atrial pressure source (p_{LA}), the mitral valve (diode), atrio-ventricular valve resistance (R_{LAV}), and atrio-ventricular inductance (L_{AV}). It also includes the aortic valve (diode), ventriculo-arterial valve resistance (R_{av}), ventrictulo-arterial inductance (L_{Va}), and a time-varying left ventricle elastance function (E(t)). The inductances allow for simulation of blood flow inertia, and the time-varying elastance accounts for ventricular contractivity changes as the ventricle contracts and relaxes.

The aorta was realistically modeled to include the aortic arch and four subordinate vessels: right subclavian artery, right carotid artery, left carotid artery, and left subclavian artery (Figure 3.4.15). Parameter values for the heart and these vessels appear in Tables 3.47 and 3.48 for rest and exercise conditions. The time-varying elastance function has been diagrammed in Figure 3.4.16. The authors stated that, if the elastance function is normalized with a maximum value and the time from the onset of systole to the appearance of maximum elastance, the shape of the elastance funtions remains the same and can be used for different conditions of contractability, vascular loading, heart rate, and heart disease.

Intraventricular pressure is related to ventricular volume through the elastance:

$$p_{LV}(t) = E(t)\,[V_{LV}(t) - V_{LV}(0)] \qquad (3.4.51)$$

where $p_{LV}(t)$ is ventricular pressure in N/m^2; $E(t)$ is left ventricle elastance in N/m^5 (the inverse of compliance); $V_{LV}(t)$ is ventricular volume in m^3; $V_{LV}(0)$ is the basic volume of the ventricle in m^3.

When left ventricular pressure rises above aortic pressure, the aortic valve opens and blood flows into the aorta and arterial system. This is systole. Aortic flow depends upon the pressure difference between left ventricle and aorta. Ventricle and aorta are closely coupled during this time. Aortic pressure was given as:

$$\begin{aligned} p_a(t) &= E(t)\,[V_{LV}(t) - V_{LV}(0)] - \dot{V}_a(t) R_{av} - \ddot{V}_a L_{Va} \\ &= E(t)\,[V_{LV}(t_{ao}) - \int_{tao}^{t} \dot{V}(s)\,ds - V_{LV}(0)] \\ &\quad - \dot{V}_a(t) R_{av} - \ddot{V}_a L_{Va} \end{aligned} \qquad (3.4.52)$$

where $p_a(t)$ is aortic inlet pressure in N/m^2; $E(t)$ is the time-varying ventricular elastance function in N/m^5; $V_{LV}(t)$ is the time-varying ventricular volume in m^3; $V_{LV}(0)$ is the ventricular volume remaining after emptying in m^3; $\dot{V}_a(t)$ is the aortic volumetric blood flow rate in m^3/sec; R_{av} is the aortic valve resistance in $N \cdot sec/m^5$; $\ddot{V}_a$ is aortic volume acceleration in m^3/sec^2; L_{Va} is the ventricle to aorta inertance in $N \cdot sec^2/m^5$; t_{ao} is the time when the aortic valve opens in sec; t is general time in sec; s is a dummy variable in sec.

During systole, when blood flows into the aorta, the authors used a Neumann boundary condition[1] to solve the coupled upstream ventricular conditions to the downstream three-dimensional finite element model of the aorta. During diastole, the

aortic valve is mostly closed, and there is no flow into the aorta. The authors used a Dirichlet boundary condition[1] in that case. They used a Dirichlet boundary condition for the short time during the transient closing of the aortic valve when there is retrograde aortic flow back into the ventricle.

They also included cardiac atrial action to fill the ventricle. When the mitral valve was opened, left atrial pressure was given as:

$$p_{LA}(t) = E(t)\,[V_{LV}(t) - V_{LV}(0)] + \dot{V}_{oLA}(t)R_{LAV} + \ddot{V}_{LA}\,L_{AV}$$

$$= E(t)\,[V_{LV}(t_{mo}) - \int_{tmo}^{t} \dot{V}_{oLA}(s)\,ds - V_{LV}(0)]$$

$$+ \dot{V}_{oLA}(t)\,R_{LAV} + \ddot{V}_{LA}\,L_{AV} \qquad (3.4.53)$$

where $p_{LA}(t)$ is left atrial pressure in N/m^2; $\dot{V}_{oLA}(t)$ is atrial blood flow rate in m^3/sec^2; L_{AV} is the atrial-to-ventricular inertance in $N\cdot sec^2/m^5$; t_{mo} is the time when the mitral valve opens in sec. All other symbols are as defined previously.

The authors assumed that blood was a Newtonian fluid with a density of 1060 kg/m^3 (1.06 g/m^3) and a dynamic viscosity of 4 g/m·sec (0.04 dynes·sec/cm^2). Blood vessel walls were modeled as linear elastic material with Poisson's ratio[2] of 0.5, wall density of 1000 kg/m^3 (1.0g/cm^3), and a thickness of 10^{-3}m (0.1 cm). They approximated physical parameters from:

$$t_{max} = T_c / 3 \quad \text{at rest} \qquad (3.4.54\,a)$$

$$t_{max} = T_c / 2 \quad \text{during exercise} \qquad (3.4.54b)$$

$$E_{max} = \frac{\gamma_c}{T_c} R_p \qquad (3.4.55)$$

$$V_{LV}(0) = V_s - \frac{0.9\, p_{syst}}{E_{max}} \qquad (3.4.56)$$

where t_{max} is the time from the beginning of systole to the maximum elastance value in sec; T_c is the cardiac cycle period in sec; γ_c is a dimensionless parameter that varies between 1 and 2; R_p is the total resistance of the systemic circulation in N·sec/m^5; V_s is the end-systolic ventricular volume in m^3; p_{syst} is the ventricular systolic pressure in N/m^2. Numerical values appear in Tables 3.4.7 and 3.4.8.

The model was run for both resting and exercise conditions. Flows and pressures were calculated for the aortic inlet, descending thoracic aorta, right and left carotid arteries, and right and left subclavian arteries. Flow rates for aortic inlet and right carotid artery inlet are shown in Figures 3.4.17 and 3.4.18. Additional flow and pressure results can be found in the original article (Kim et al., 2009).

Table 3.4.7 Inlet Conditions for the Aorta Model (Kim et al., 2009)

R_{LAV}		10×10^5 N·sec/m^5	(10 dyne·sec/cm^5)
L_{AV}		0.67×10^5 N·sec^2/m^5	(0.67 dyne ·sec^2/cm^5)
R_{av}		10×10^5 N·sec/m^5	(10 dyne·sec/cm^5)
L_{Va}		0.69×10^5 N·sec^2/m^5	(0.69 dyne ·sec^2/cm^5)
E_{max}		2.7×10 N/m^5	(2.0 mmHg/cm^3)
$V_{LV}(0)$		-33×10^{-6} m^3	(-33 cm^3)
p_{LA}	rest	1870 N/ m^2	(14 mm Hg)
	exercise	1870 N/ m^2	(14 mm Hg)

t_{max}	rest	0.32 sec	(0.32 sec)
	exercise	0.3 sec	(0.3 sec)
T_c	rest	0952 sec	(0.952 sec)
	exercise	0.6 sec	(0.6 sec)

Table 3.4.8 Outlet conditions for the Aorta Model (Kim et al., 2009)

	Rest	Exercise
Right-Subclavian Artery		
R_{pa}	1.04×10^8 N·sec/m^5 (1040 dynes·sec/cm^5)	1.04×10^8 N·sec/m^5 (1040 dynes·sec/cm^5)
C_a	8.74×10^{-10} m^5/N (8.74×10^{-5}cm^5/dyne)	8.74×10^{-10} m^5/N (8.74×10^{-5} cm^5/dyne)
R_{da}	1.63×10^9 N·sec/m^5 (16300 dyne·sec/cm^5)	1.63×10^9 N·sec/m^5 (16300 dyne·sec/cm^5)
Right and Left Carotid Arteries		
R_{pa}	1.18×10^8 (1180)	1.18×10^8 (1180)
C_a	7.70×10^{-10} (7.70×10^{-5})	7.70×10^{-10} (7.70×10^{-5})
R_{da}	1.84×10^9 (18400)	1.84×10^9 (18400)
Left Subclavian Artery		
R_{pa}	9.70×10^7 (970)	9.70×10^7 (970)
C_a	9.34×10^{-10} (9.34×10^{-5})	9.34×10^{-10} (9.34×10^{-5})
R_{da}	1.52×10^9 (15200)	1.52×10^9 (15200)
Descending Thoracic Aorta		
R_{pa}	1.88×10^7 (188)	7.5×10^6 (75)
C_a	4.82×10^9 (4.82×10^{-4})	4.82×10^{-9} (4.82×10^{-4})
R_{da}	2.95×10^8 (2950)	1.27×10^8 (1270)

Symbols for R_{pe}, R_{da}, and C_a appear in Figure 3.4.15. Units for R_{pa} and R_{da} are $N \cdot sec/m^5$. Values in parentheses are original units in $dyne \cdot sec/cm^5$.

Units for C_a are m^5/N. Values in parentheses are original units in $cm^5/dyne$.

Footnotes

1) A Neumann boundary condition exists when there is a specified flow across a boundary. A Dirichlet boundary condition exists when the specified boundary condition is a value of the function. Here, the Dirichlet condition means that a pressure value is specified when the aortic valve closed and there is no flow.

2) As a material is elastically lengthened longitudinally, it concomitantly contracts laterally. The ratio of lateral unit deformation to linear unit deformation within the elastic limit is known a Poisson's ratio.

References

Kim, H.J., I.E. Vignon-Clementel, C. A. Figueroa, J. F. LaDisa, K.E. Jansen, J. A. Feinstein, and C. A. Taylor, 2009, On Coupling a Lumped Parameter Heart Model and a Three-Dimensional Finite Element Aorta Model, *Ann. Biomed. Engr*. 37(11): 2153-2169.

Vignon-Clementel, I. E., C. A. Figueroa, K. E. Jansen, and C. A. Taylor, 2010, Outflow Boundary Conditions for Three-Dimensional Simulations of Non-Periodic Blood Flow and Pressure Fields in Deformable Arteries, *Comput. Meth. Biomech. Biomed. Engr*.

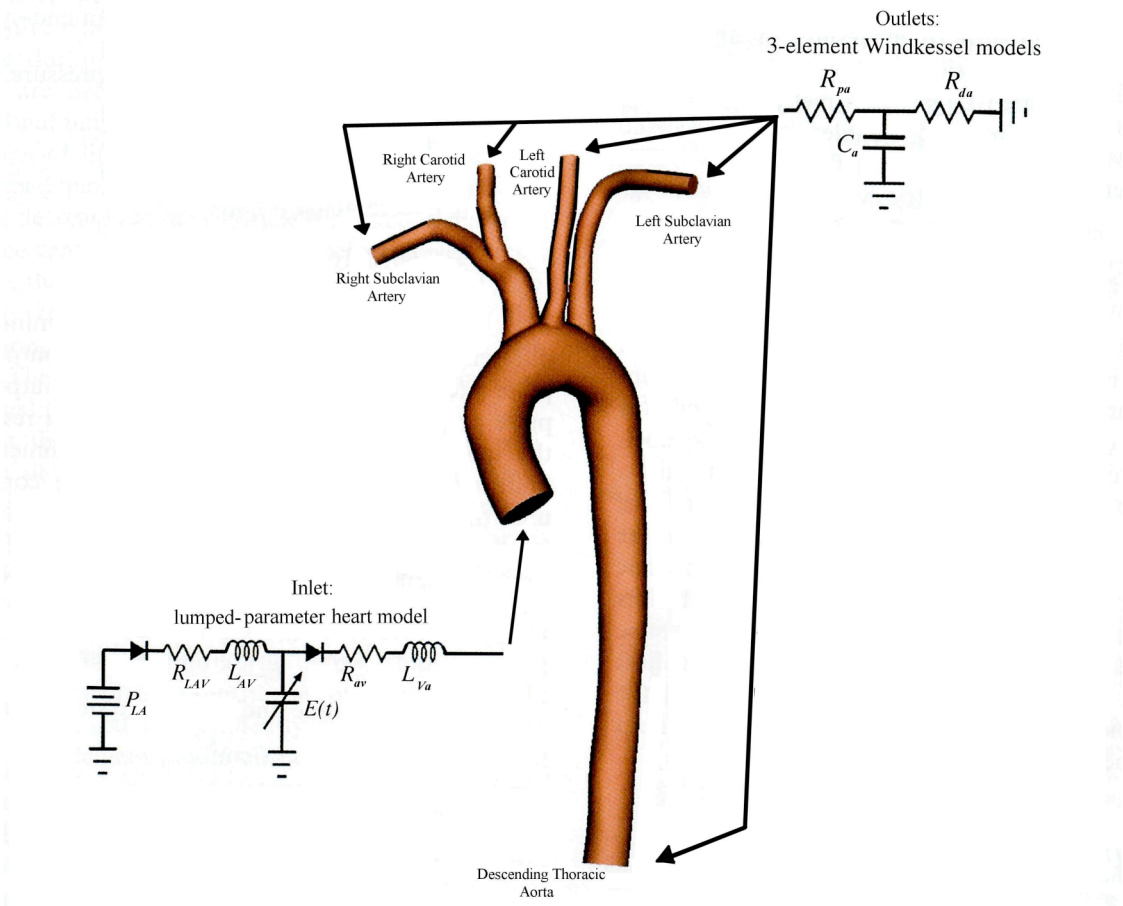

Figure 3.4.15. Lumped-parameter heart and blood vessel models linked to upstream and downstream finite-element model of the aorta (Kim et al., 2009).

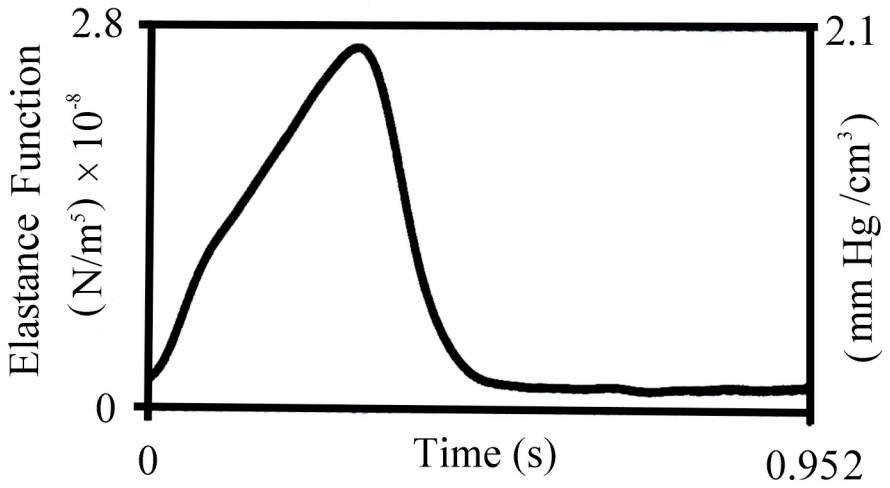

Figure 3.4.16. Time varying elastance function for the left ventricle used in the aorta model (Kim et al., 2009).

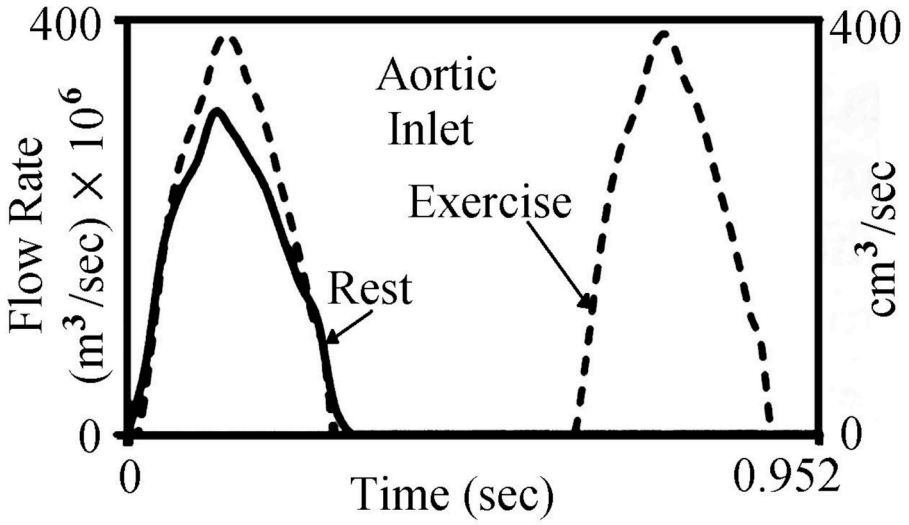

Figure 3.4.17. Time varying flow rate model results at the inlet to the aorta for rest and exercise (Kim et al., 2009).

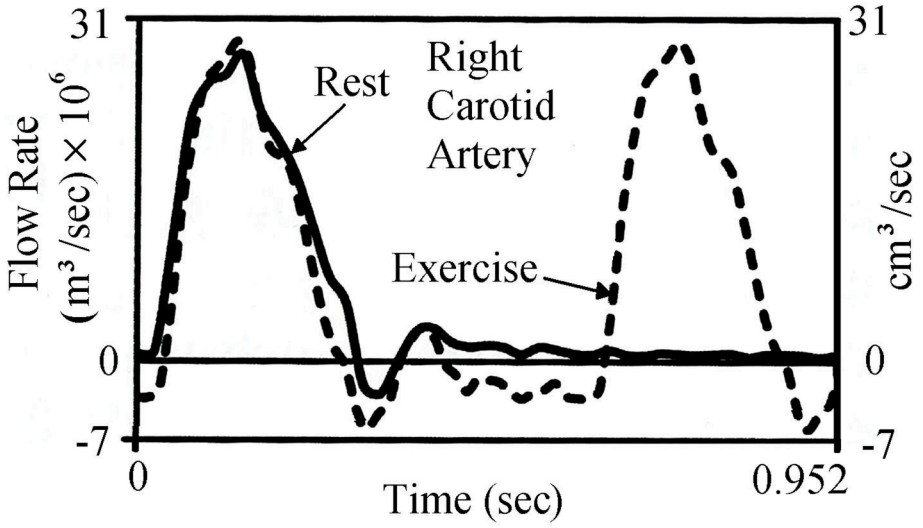

Figure 3.4.18. Time varying flow rate model results at the inlet of the right carotid artery (Kim et al., 2009). Notice that there is a period of backflow that occurs during diastole. Additional flows and pressure results can be found in the original article.

Example 3.4.6.1 **Carotid Blood Pressure.** Calculate blood pressure in the right carotid artery 0.1 sec after the beginning of systole.

Solution

The model itself can be used to calculate right carotid artery blood pressure as a function of time, and in the original article by Kim et al., (2009) are presented graphs of arterial pressures with time. Nonetheless, right carotid arterial pressure can be calculated using their lumped-parameter carotid artery model (Figure 3.4.15) plus minimal flow rate data given in Figure 3.4.18.

From the model in Figure 3.4.15, it can be seen that the artery is modeled as a parallel combination of R_{da} and C_a in series with the resistance R_{pa}. The question becomes one of determining what inlet pressure is required to push the flow rate appearing in Figure 3.4.18 through this simple component network?

The total inlet pressure (p) equals the pressure (p_1) appearing at the junction of R_{pa}, R_{da}, and C_a plus the pressure drop ($\dot{V}_{TOT}R_{pa}$) across R_{pa}:

$$p = p_1 + R_{pa}\,\dot{V}_{TOT}$$

Realizing that the flow $\dot{V}_{TOT} = \dot{V}_{Ca} + \dot{V}_{Rda}$

This same equation can be obtained from Kirchoff's node equation.

Flow through R_{da} ($\dot{V}_{Rda}$) is just:

$$\dot{V}_{Rda} = p_1/R_{da}$$

and flow through the capacitor is:

$$\dot{V}_{Ca} = C_a \frac{dp_1}{dt}$$

Thus,

$$\dot{V}_{TOT} = C_a \frac{dp_1}{dt} + \frac{p_1}{R_{da}}$$

From Figure 3.4.18, total flow ($\dot{V}_{TOT}$) can be measured at the time of 0.1 sec as 26.5 $\times 10^{-6}$ m^3sec, and the flow is not steady, but rising. The rising is important because there is time involved in the equation above. To simplify this problem somewhat, it will be assumed that $\dot{V}_{TOT}$ rises linearly with time. This approximation can be seen to be nearly correct based on the shape of the curve in Figure 3.4.18.

Note also that there is a short time delay before flow begins to increase. Again, to simplify the problem, time will be shifted by the amount of this delay (measured from the Figure as 0.0216 sec). Thus, 0.1 sec in the original time scale becomes 0.0784 sec in the shifted time scale.

From the assumption of linearly increasing $\dot{V}_{TOT}$:

$$\dot{V}_{TOT}\ (t) = kt$$

$$\dot{V}_{TOT}\ (0.0784 \text{ sec}) = k\ (0.0784 \text{ sec}) = 26.5 \times 10^{-6}\ m^3/\text{sec}$$

$$k = 3.38 \times 10^{-4}\ m^3/\text{sec}^2$$

This makes the first order differential equation for p_1:

$$C_a \frac{dp_1}{dt} + \frac{p_1}{R_{da}} = kt$$

$$\frac{dp_1}{dt} + \frac{1}{\tau} p_1 = \frac{kt}{C_a}$$

where $\tau = C_a R_{da}$. This differential equation requires a complementary solution and a particular solution. The complementary solution (p_{1c}) is to be found first. The auxiliary differential equation is:

$$\frac{dp_{1c}}{dt} + \frac{1}{\tau}\, p_{ic} = 0$$

or,

$$\frac{dp_{1c}}{p_{ic}} = \frac{1}{\tau}\, dt$$

integrating,

$$\ln p_{ic} = \frac{t}{\tau} + A$$

or,

$$p_{ic} = Ae^{-t/\tau}$$

where A is a constant of integration to be found later based on initial conditions.

The particular solution (p_{1p}) to the differential equation requires a form for p_{1p} that includes a term with time involved. We can try a function of the form:

$$p_{1p} = at + b$$

This makes our original differential equation:

$$\frac{dp_{1p}}{dt} + \frac{1}{\tau} p_{1p} = a + \frac{at}{\tau} + \frac{b}{\tau} = \frac{k}{C_a} t$$

Collecting terms on both sides of the equation involving t^1:

$$\frac{a}{\tau} = \frac{k}{C_a}$$

$$a = \frac{k\tau}{C_a}$$

Collecting terms on both sides of the equation involving t^o :

$$a + \frac{b}{\tau} = 0$$

$$b = -\frac{k\tau^2}{C_a}$$

Thus,

$$p_{1p} = \frac{k\tau\, t}{C_a} - \frac{k\tau^2}{C_a}$$

Note that each term in this equation is dimensionally homogeneous with the units N/m^2.

Total p_1 equals $p_{ic} + p_{1p}$:

$$p_1 = Ae^{-\tau/\tau} + \frac{k\tau\, t}{C_a} - \frac{k\tau^2}{C_a}$$

or,

$$p = Ae^{-t/\tau} + \frac{k\,\tau\, t}{C_a} - \frac{k\tau^2}{C_a} + R_{pa}\dot{V}_{TOT}$$

To solve for the value of A, we can assume that p=0 when t=0. This is true for both rest and exercise as long as we use the time offset described previously. Exercise flow rates can be seen to be negative prior to this delay, and this implies negative pressures.

Putting initial conditions into the previous equation:

$$0 = Ae^{-0} + \frac{k\tau(0)}{C_a} - \frac{k\tau^2}{C_a} + R_{pa}\dot{V}_{TOT}$$

$$0 = A + 0 - \frac{k\tau^2}{C_a} + R_{pa}\dot{V}_{TOT}$$

$$A = \frac{k\tau^2}{C_a} - R_{pa}\dot{V}_{TOT}$$

Which gives:

$$p = \left(\frac{k\tau^2}{C_a} - R_{pa}\dot{V}_{TOT}\right) e^{-t/\tau} + \frac{k\tau\, t}{C_a} - \frac{k\tau^2}{C_a} + R_{pa}\,\dot{V}_{TOT}$$

$$p = \frac{k\tau}{C_a}\left[t - \tau\,(1 - e^{-t/\tau})\right] + R_{pa}\dot{V}_{TOT}\,(1 - e^{-t/\tau})$$

Calculating,

$$\tau = R_{da}C_a = (1.84\times10^{9}\ \frac{\mathrm{N\cdot sec}}{\mathrm{m^5}})(7.70\times10^{-10}\ \frac{\mathrm{m^5}}{\mathrm{N}})$$

$$= 1.4168\ \mathrm{sec}$$

$$R_{pa}\dot{V}_{TOT} = (1.18\times10^{8}\ \mathrm{N\cdot sec/m^5})(26.5\times10^{-6}\ m^3/\mathrm{sec})$$

$$= 3127\ \mathrm{N/m^2}$$

$$(1 - e^{-t/\tau}) = 1 - e^{-(0.0784/1.4168)} = 0.05383$$

$$\frac{k\tau}{C_a} = \frac{(3.38\times10^{-4}\ m^3/\mathrm{sec^2})\,(1.4168\,\mathrm{sec})}{(7.70\times10^{-10}\ m^5/N)} = 621{,}920\ \frac{\mathrm{N}}{\mathrm{m^2\cdot sec}}$$

Thus, p at t=0.078 sec (at 0.1sec real time) is:

$$p = 621{,}920\ \frac{\mathrm{N}}{\mathrm{m^2\cdot sec}}[0.0784\ \mathrm{sec} - (1.4168\ \mathrm{sec})\ (0.05383)]$$

$$+ 3127\ \frac{\mathrm{N}}{\mathrm{m^2}}\ (0.05383)$$

$$p = 1495\ \mathrm{N/m^2}$$

Remark: This value is only about one-tenth of the carotid artery pressure given in the original article at a time of 0.1 sec. This discrepancy can be ascribed to: 1) flow and pressure at the inlet to the carotid artery are periodic; the analysis in this example did not account for periodicity, 2) it took several cardiac cycles for the Kim et al. model to converge to a periodic solution (Vignon-Clementel et al., 2010), and 3) carotid artery

compliance induces a phase angle between pressure and flow that is not completely accounted for in this example.

Add to List of Symbols

C_a	arterial compliance, m^5/N
$E(t)$	left ventricle elastance, N/m^5
E_{max}	maximum value of ventricular elastance, N/m^5
L_{AV}	atrial-to-ventricular inertance, $N \cdot sec^2/m^5$
L_{Va}	ventriculo-arterial inertance, $N \cdot sec^2/m^5$
p_{syst}	ventricular systolic pressure, N/m^2
R_{da}	arterial resistance term, $N \cdot sec/m^5$
R_{pa}	arterial resistance term, $N \cdot sec/m^5$
s	dummy variable, sec
T_c	time between heart beats, sec
t_{ao}	time when aortic valve opens, sec
t_{max}	time when maximum ventricular elastance occurs, sec
t_{mo}	time when mitral valve opens, sec
$\dot{V}_a$	aortic flow rate, m^3/sec
$\ddot{V}_a$	aortic volume acceleration, m^3/sec^2
$\ddot{V}_{LA}$	atrial volume acceleration, m^3/sec^2
γ_c	dimensionless cardiac parameter

Add to Index:

arterial

mitral valve

Subclavian artery

Systole

Ventricle, left